NACA RM L55C09

NACA

RESEARCH MEMORANDUM

FLIGHT INVESTIGATION OF THE SUPERSONIC AREA RULE FOR A STRAIGHT WING-BODY CONFIGURATION AT MACH NUMBERS BETWEEN 0.8 AND 1.5

By Sherwood Hoffman, Austin L. Wolff, and Maxime A. Faget

Langley Aeronautical Laboratory
Langley Field, Va.

NATIONAL ADVISORY COMMITTEE FOR AERONAUTICS

WASHINGTON

April 29, 1955
Declassified September 14, 1959

NACA RM L55C09

NATIONAL ADVISORY COMMITTEE FOR AERONAUTICS

RESEARCH MEMORANDUM

FLIGHT INVESTIGATION OF THE SUPERSONIC AREA RULE FOR A STRAIGHT WING-BODY CONFIGURATION AT MACH NUMBERS BETWEEN 0.8 AND 1.5

By Sherwood Hoffman, Austin L. Wolff, and Maxime A. Faget

SUMMARY

An investigation of the supersonic area rule has been conducted by rocket-propelled model tests of zero-lift models of a straight wing-body configuration through a range of Mach number from 0.8 to 1.5 and Reynolds number from 5×10^6 to 12×10^6. The body of the basic configuration was modified with axial symmetrical indentations according to area-rule considerations for low wave drag at design Mach numbers of 1.10 and 1.41. The indentations were designed using a short method (given in appendix) that greatly simplified the work. Each configuration had at its respective design Mach number the same distribution of cross-sectional area as the basic body alone. The basic body was parabolic having a frontal area equal to 0.0606 that of the total wing plan-form area. The wing had an aspect ratio of 3.04, taper ratio of 0.394, 0° of sweep along the 75-percent chord line, and an NACA 65A004.5 airfoil section in the free-stream direction.

Both the Mach number 1.10 and 1.41 indentations reduced the wave drag of the basic configuration at transonic speeds with the greater reduction being obtained from the Mach number 1.10 indentation. The beneficial effects from the indentations decreased with increasing Mach number until Mach number 1.3, above which no benefits were obtained from either indentation. Both indented configurations had the same drag-rise above Mach number 1.15. The theoretical wave drags of the configurations were useful in showing the relative merits of the different indentations.

INTRODUCTION

The transonic area rule of reference 1 provides a simple and effective means for designing high-speed aircraft for low wave drag near the speed of sound. Investigations of the transonic area rule (refs. 1 to 11)

for several wing-body configurations have shown that a substantial reduction in the drag rise near Mach number 1.0 may be obtained by modifying or designing an airplane to have a cross-sectional area distribution that is conducive to low drag. A convenient type of modification is a fuselage indentation for Mach number 1.0, which effectively cancels the exposed wing cross-sectional areas normal to the axis of symmetry. However, recent investigations (refs. 2 and 11, for example) have shown that the beneficial effects obtained from such indentations decrease with increasing Mach number and eventually produce an unfavorable effect on the drag. This effect is particularly acute on straight wing-body combinations where the indentations result in considerable necking down of the fuselage causing high body slopes at the wing-body juncture.

The concept of the transonic area rule has been extended to supersonic speeds (refs. 12 to 15) in an attempt to provide area distributions for low wave drag at supersonic speeds as well as transonic speeds. This paper presents an investigation of the supersonic area rule for a straight wing-body configuration which was optimized with symmetrical body indentations (according to ref. 13) for design Mach numbers of 1.10 and 1.41. The wing had an aspect ratio of 3.04, taper ratio of 0.394, 0° of sweep along the 75-percent chord line, and an NACA 65A004.5 airfoil section in the free-stream direction. The unmodified fuselage was parabolic having a frontal area equal to 0.0606 that of the total wing planform area.

The models were flight tested at the Langley Pilotless Aircraft Research Station at Wallops Island, Va. The tests of the indented configurations covered a continuous range of Mach number from 0.8 to 1.5 with corresponding Reynolds number from 5×10^6 to 12×10^6, based on wing mean aerodynamic chord. The experimental results are compared with the theoretical wave drags of the configurations tested through most of the Mach number range.

SYMBOLS

A	cross-sectional area
a	tangential acceleration
C_D	total drag coefficient, based on S_w
$\bar{c}$	mean aerodynamic chord of wing
g	acceleration due to gravity

L	length of body
M	free-stream Mach number
q	free-stream dynamic pressure
R	Reynolds number, based on $\bar{c}$
S_w	total wing plan-form area
W	weight of model during deceleration
x	station measured from body nose
γ	angle between flight path and horizontal
Φ	angle of roll of configuration with respect to Mach planes. At 0° of roll the Mach planes are perpendicular to the wing plane.

MODELS

Details and dimensions of the models tested are given in figure 1 and tables I to IV. Photographs of the models are presented as figure 2.

The basic configuration, model A, was originally tested for the investigation of reference 16 and consisted of a straight wing on a parabolic body with two vertical stabilizing fins. The parabolic body profile was formed by two parabolas joined at the maximum diameter (40-percent body station) and had an overall fineness ratio of 10.0. The straight wing had a total aspect ratio of 3.04, taper ratio of 0.394, 0° of sweep at the 75-percent chord line, and an NACA 65A004.5 airfoil in the free-stream direction. The ratio of body frontal area to total wing plan-form area was 0.0606.

Configurations B and C were obtained by indenting the parabolic body of the basic configuration for design Mach numbers of 1.10 and 1.41, respectively. As is stated in reference 13 for radially symmetrical modifications, the area used for the optimum indentation is obtained by averaging the frontal projection of wing areas cut by Mach planes at all angles of roll (Φ) of the Mach planes with respect to the configuration. For symmetrical models, only the average areas between 0° and 90° have to be considered. Since such computations require considerable time, a short method has been devised from which the average projected wing areas used for indenting the body can be

obtained directly. This method is outlined in the appendix and shows how average supersonic area distributions could be obtained by substituting a series of hoops for the wing. The resulting area distributions for models B and C, at their respective design Mach numbers, were the same as the normal cross-sectional area distribution of the original parabolic body. It was assumed that the cross-sectional area of the original body did not change through the Mach number range considered. The two stabilizing fins used on models A, B, and C were neglected in determining the area distributions of the configurations because of their thin sections and high sweepback angle. Both models B and C were one-half the scale used for model A. The identation used removed about 14 percent of the volume of the original body shape.

TESTS AND MEASUREMENTS

All the models were tested at the Langley Pilotless Aircraft Research Station at Wallops Island, Va. Models A, B, and C were zero-lift rocket-propelled models that were accelerated from zero-length launchers to supersonic speeds by single-stage 6-inch ABL Deacon rocket motors. Model A, the largest of the group, was propelled by a rocket motor installed in its body; whereas, models B and C were propelled by boosters, consisting of the rocket motors with stabilizing fins (fig. 3), that separated from the models after burnout. Velocity and trajectory data were obtained from the CW Doppler velocimeter and the NACA modified SCR 584 tracking radar unit, respectively. A survey of atmospheric conditions including winds aloft was made by radiosonde measurements from an ascending balloon that was released at the time of each launching.

The flight tests covered continuous ranges of Mach number varying between Mach numbers 0.8 and 1.5. The corresponding Reynolds numbers, based on wing mean aerodynamic chord, are shown in figure 4 to vary from 9×10^6 to 25×10^6 for model A, and 5×10^6 to 12×10^6 for models B and C through the Mach number ranges covered.

The values of total drag coefficient, based on total wing plan-form area, for all the models were obtained during decelerating flight with the expression

$$C_D = -\frac{W}{qgS_w}(a + g \sin \gamma)$$

where a was obtained by differentiating the velocity-time curve from the CW Doppler velocimeter. A more complete discussion of the method for reducing the data is given in reference 17.

The error in total drag coefficient C_D was estimated to be of the order of ±0.0007 at supersonic speeds and ±0.001 at transonic speeds. The Mach numbers were determined within ±0.01 throughout the test range.

RESULTS AND DISCUSSION

The variations of total drag coefficient C_D with Mach number for the basic and indented wing-body configurations are shown in figure 5. The drags presented for model A and the fins were published as part of an earlier investigation in reference 16. The curves shown in this figure represent the basic drag data from the flight tests and are not intended for comparison due to the relatively different surface roughness of the models (obtained from changing model scale) and the different Reynolds number ranges of the tests.

A comparison of the variation of drag rise $(C_D - C_{D_{subsonic}})$ of the models through the Mach number range is shown in figure 6. At Mach number 1.0, the drag rise of the basic configuration was reduced by 35 percent with the Mach number 1.10 indentation and by 20 percent with the Mach number 1.41 indentation. These results are in qualitative agreement with the concepts of the transonic area rule as may be seen by comparing the drag rises with the normal cross-sectional area distributions of the models in figure 7(a). Figure 6 also shows that the beneficial effects from both indentations decreased with increasing Mach number until Mach number 1.3. At higher speeds, the drag rises of the basic configuration and the two indented configurations were about the same. For the design conditions of the indented configurations, model B with the Mach number 1.10 indentation had 23 percent less drag rise than the original configuration at $M = 1.10$, while model C with the Mach number 1.41 indentation had about the same drag rise as the original configuration at $M = 1.41$. Both models B and C gave the same drag rise above $M = 1.15$. These comparisons indicate that the $M = 1.41$ indentation did not optimize the configuration at its design Mach number.

The supersonic area-rule concept of references 18 and 13 makes possible the calculation of the wave drag of slender wing-body combinations at supersonic speeds. While this theory when taken to the limit of $M = 1.0$ shows that the drag is solely dependent on the normal cross-sectional area distribution (transonic area rule of ref. 1), the magnitude of the theoretical wave drag near $M = 1.0$ is in error as is shown in references 13 to 15. At supersonic speeds, reference 13 shows that the wave drag may be determined from a series of area distributions or equivalent bodies of revolution. Each area distribution of the series is obtained from the frontal projection of the area intercepted by parallel Mach planes at a given angle of roll of the configuration with

respect to the Mach planes. The drag coefficient of the configuration is then determined from the average of the drag coefficients for all the equivalent bodies of revolution. It is important to use the series of area distributions for determining the wave drags and not the average area distributions that were employed in designing the indentations. Use of the average areas for the computations would give values that greatly underestimate the drag of the configurations. A detailed description of this method showing the evaluation of the wave drag by Fourier sine series and how to determine the wave drags over a range of Mach number is given in references 14 and 15.

Since the present models were symmetrical, only the areas between roll angles of 0° and 90° had to be considered. Some of the area distributions for the models tested are shown in figures 7(b) to 7(g). According to the convention used, the Mach planes were perpendicular to the wing plane at 0° roll. For the roll angles at which the Mach line slices were alined with the blunt leading edge and trailing edge of the wing, discontinuities appear on the slopes of the area distributions, limiting the application of the linearized theory to about Mach number 1.1 for the present case. High values of slope were assumed rather than these discontinuities in order to extend the Mach number range and determine if reasonable agreement could be obtained with the experimental drag rises at higher Mach numbers. The Fourier sine series used for calculating the drag of each equivalent body of revolution was evaluated to 24 terms and plots of these series indicated that the series were convergent. It should be noted, however, that while the series converge for the first 24 terms they may diverge when more terms are evaluated. In this regard, reference 15 suggests that 48 terms be used before establishing the convergence of the series.

The theoretical wave drag coefficients were computed for the models through a range of Mach number from 1.0 to 1.4 and are presented in figure 8. The computed wave drags in figure 8 are in general agreement with the observations made from the flight test data and lead to the same conclusions, namely that the Mach number 1.10 indentation is better than the Mach number 1.41 indentation at transonic and low supersonic speeds and that the Mach number 1.41 indentation offers little or no savings in wave drag at the design Mach number. Near Mach number 1.0, the theoretical variations are not realistic due to the limitations of the theory (ref. 13) used.

Comparisons of the theoretical wave drag coefficients and the measured drag-rise coefficients for each configuration tested are given in figure 9. The best agreement is shown for model B in both magnitude and variation. Although the agreement obtained for models A and B is poor, the deviation between the theory and test values is not greater than 20 percent in the Mach number range from 1.1 to 1.4. The agreement obtained in this Mach number range is better than what was expected in

view of the fact that the theory does not apply above $M = 1.1$ because the leading edge of the wing is blunt. However, from the standpoint of the configuration as a whole, the theory was useful in showing the relative merits of the different indentations.

CONCLUSIONS

The results of an investigation of the supersonic area rule by rocket-propelled model tests of zero-lift models of a straight wing-body combination having body indentations for design Mach numbers of 1.10 and 1.41, tested through a range of Mach number from 0.8 to 1.5 indicate the following conclusions:

1. Both the Mach number 1.10 and 1.41 indentations reduced the wave drag of the basic configuration at transonic speeds with the greater reduction being obtained from the Mach number 1.10 indentation. Both indented configurations had the same drag rise above Mach number 1.15.

2. The beneficial effects from the indentations decreased with increasing Mach number until Mach number 1.3, above which no benefits were obtained from either the Mach number 1.10 or 1.41 indentations.

3. The theoretical wave drags of the configurations were useful in showing the relative merits of the indentations.

Langley Aeronautical Laboratory,
National Advisory Committee for Aeronautics,
Langley Field, Va., February 25, 1955.

APPENDIX

A SHORT METHOD OF DETERMINING THE AVERAGE AREA DISTRIBUTION FOR AIRCRAFT AT SUPERSONIC SPEEDS

By Maxime A. Faget

The equivalent average area body for supersonic speeds is determined from slices made at the Mach angle. The area used is the frontal projection of the average area cut by a Mach plane as the aircraft configuration is rotated about its axis a full 360° relative to the Mach plane.

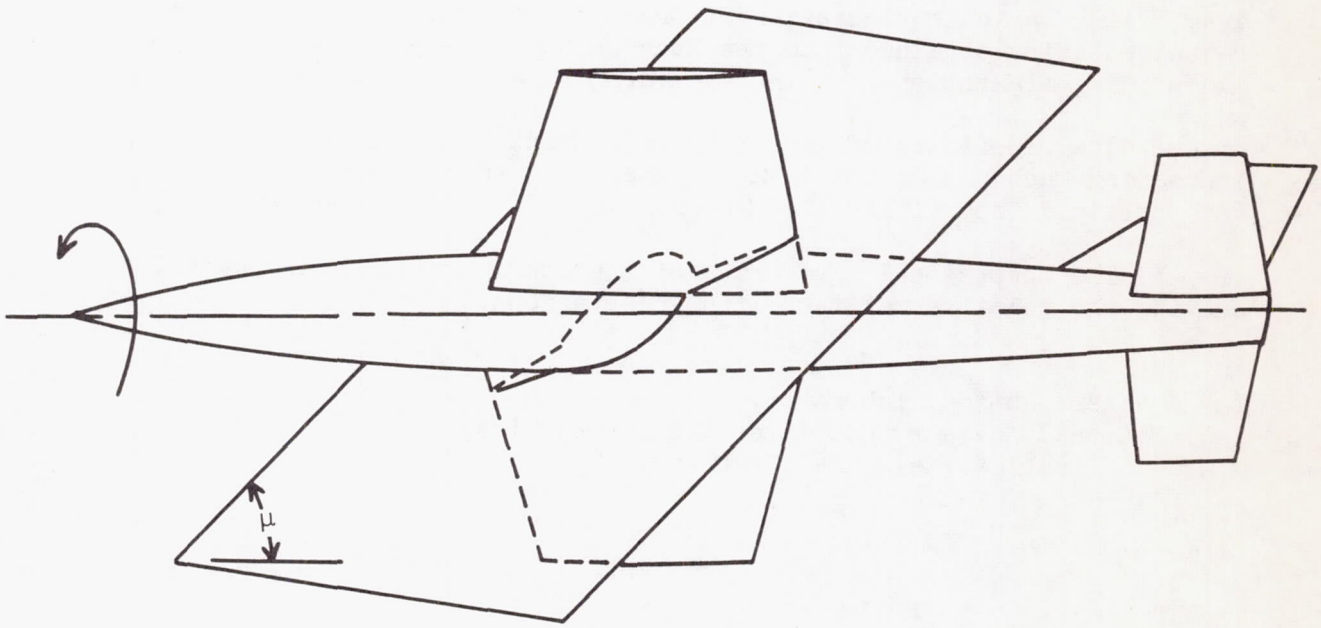

The basis of the method to be described is to construct an imaginary model of the configuration that represents all rotational positions. Thus, one plane slanted at the Mach angle will cut an area that is already averaged for all positions of relative roll between the actual configuration and the cutting plane. This imaginary model consists of a body of revolution representing the original fuselage surrounded by a number of hoops representing wings, nacelles, tail fins, and so forth, external to the fuselage. The axial distribution of cross-sectional area of the body of revolution is equal to that of the original fuselage, and the hoops represent the axial distribution of cross-sectional area

of the original wings, nacelle tail fins, and so forth. The radius of each hoop is equal to the mean distance from the airplane center line of the portion of wing, nacelle, tail fin, and so forth, that the hoop represents. Thus, a wing may be divided into 10 spanwise portions. Each portion would then be converted into a hoop equal to it in cross-sectional area distribution and with a radius equal to the mean distance of the panel from the center line.

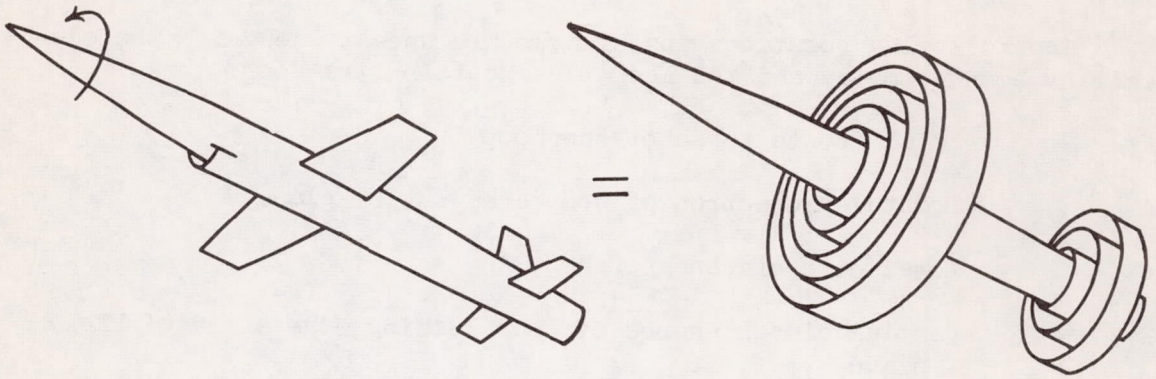

The hoops thus obtained, which are called parent hoops, are then subdivided into smaller elementary hoops in order that the variation of cross-sectional area distribution may be introduced into the computational procedure. Each family of hoops thus obtained has the same radius as its parent hoop. For convenience, these elementary hoops are made to have equal frontal area and rectangular sections, but various chord lengths.

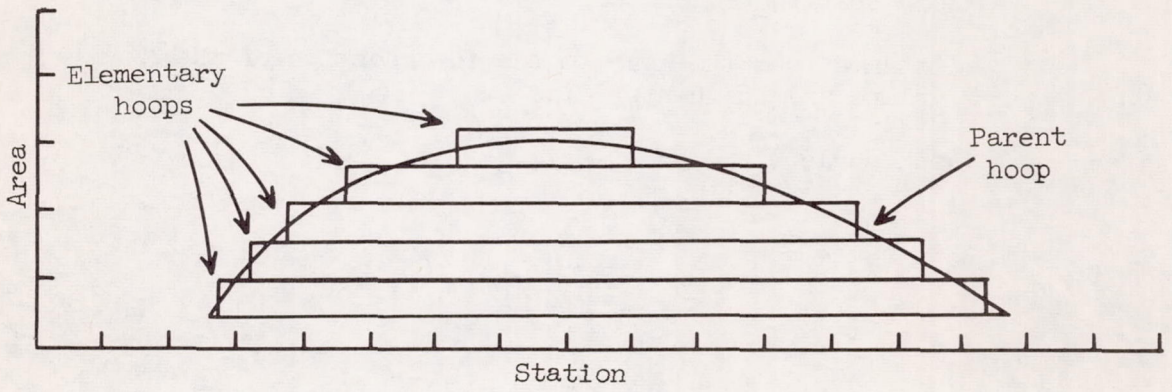

Thus, these new hoops may be described by leading-edge station, trailing-edge station, and hoop radius. It is not necessary to designate the hoop thickness as this is fixed by the fact that all hoops are of equal frontal area. Thus, the thickness is inversely proportional to hoop radius (hoops in the same family have the same thickness). With hoops of this type geometry, a simple relationship exists between the projected frontal area of the hoop which is cut by the Mach plane and the relative positions of the Mach plane and the hoop, so that rapid computation of the areas may be carried out.

The following notations and symbols are used to describe the elementary hoop geometry and the Mach plane cutting the hoop:

A^*	total frontal area of the hoop
A	frontal projection of hoop area cut by plane
C	total circumference of hoop
C_{LE}	partial circumference of hoop leading edge ahead of Mach plane
C_{TE}	partial circumference of hoop trailing edge ahead of Mach plane
R	radius of the hoop
$R' = \frac{R}{\tan \mu}$	
L	hoop leading-edge station
T	hoop trailing-edge station
X	distance from the nose to the intersection of the Mach plane and the center line
μ	Mach angle

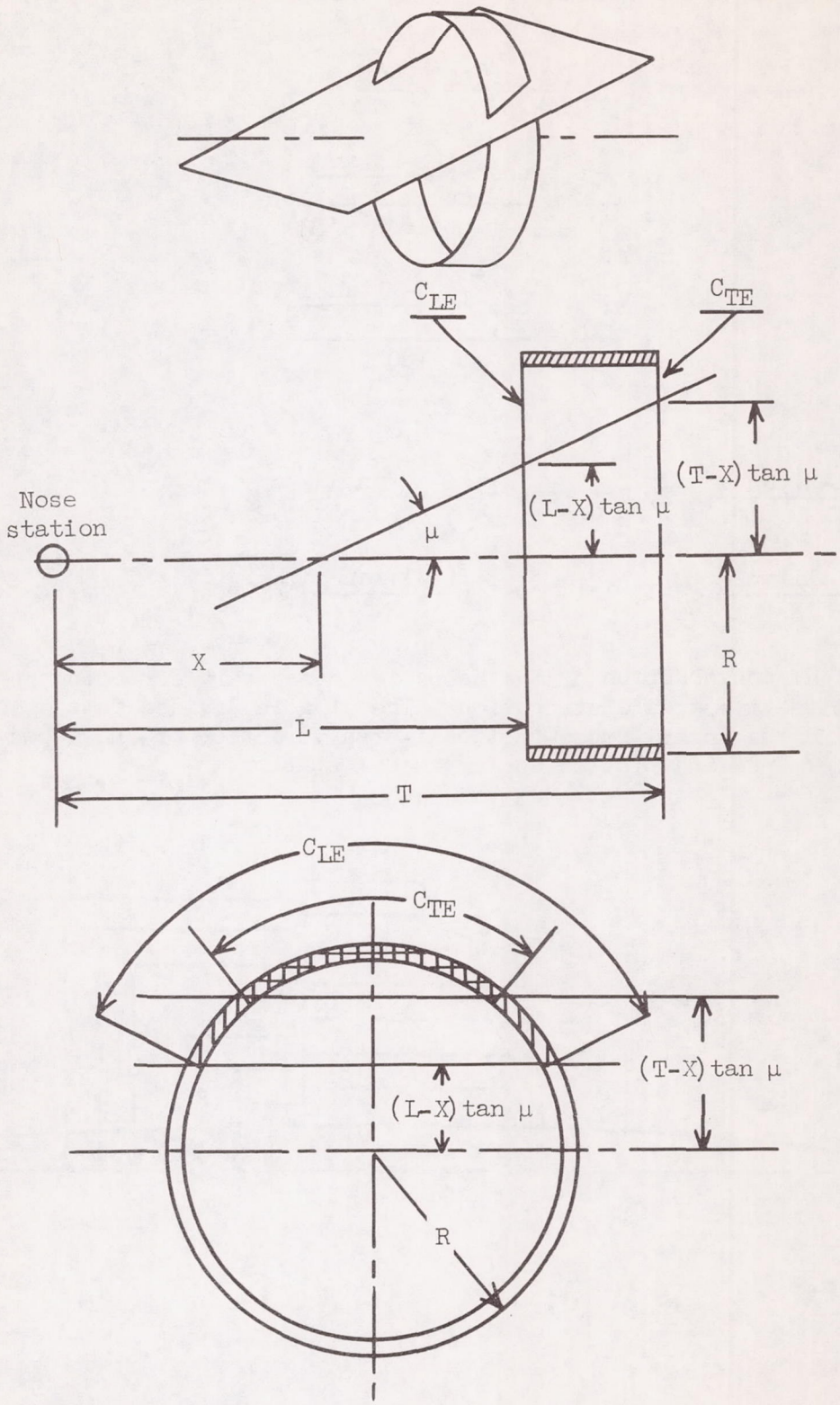
C_{LE}
C_{TE}
$(T-X)\tan\mu$
$(L-X)\tan\mu$
Nose station
μ
X
L
T
R
C_{LE}
C_{TE}
$(T-X)\tan\mu$
$(L-X)\tan\mu$
R

From the geometry in the preceding sketch, the following may be deduced:

$$\frac{A}{A^*} = \frac{C_{LE}}{C} - \frac{C_{TE}}{C} \tag{1}$$

$$\frac{C_{LE}}{C} = \frac{\cos^{-1}\left(\frac{(L-X)\tan\mu}{R}\right)}{180} \tag{2}$$

$$\frac{C_{TE}}{C} = \frac{\cos^{-1}\left(\frac{(T-X)\tan\mu}{R}\right)}{180} \tag{3}$$

Note:

when $\frac{(L-X)\tan\mu}{R} > 1$, let $\cos^{-1}\left(\frac{(L-X)\tan\mu}{R}\right) = 0$

when $\frac{(L-X)\tan\mu}{R} < -1$, let $\cos^{-1}\left(\frac{(L-X)\tan\mu}{R}\right) = 180$

Actual construction of the hoops is unnecessary for computation of the effective area distribution. The wing is divided into spanwise panels and the normal cross-sectional-area variation of these panels is then determined and plotted against model station.

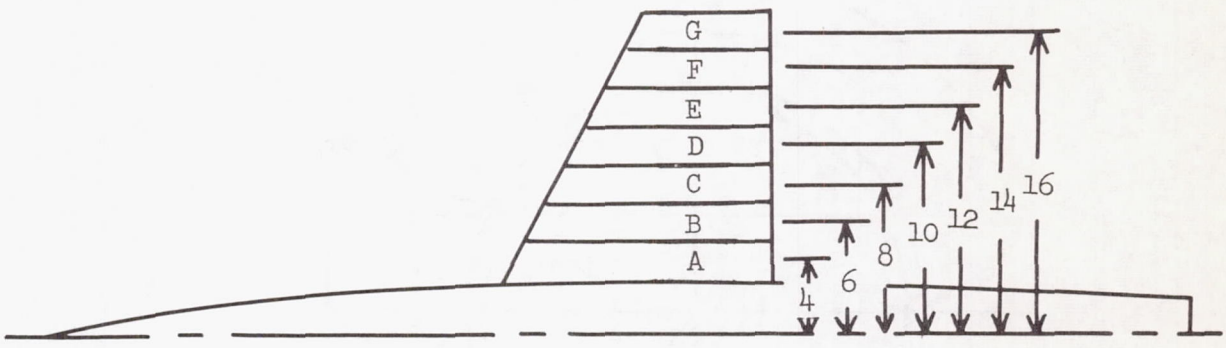

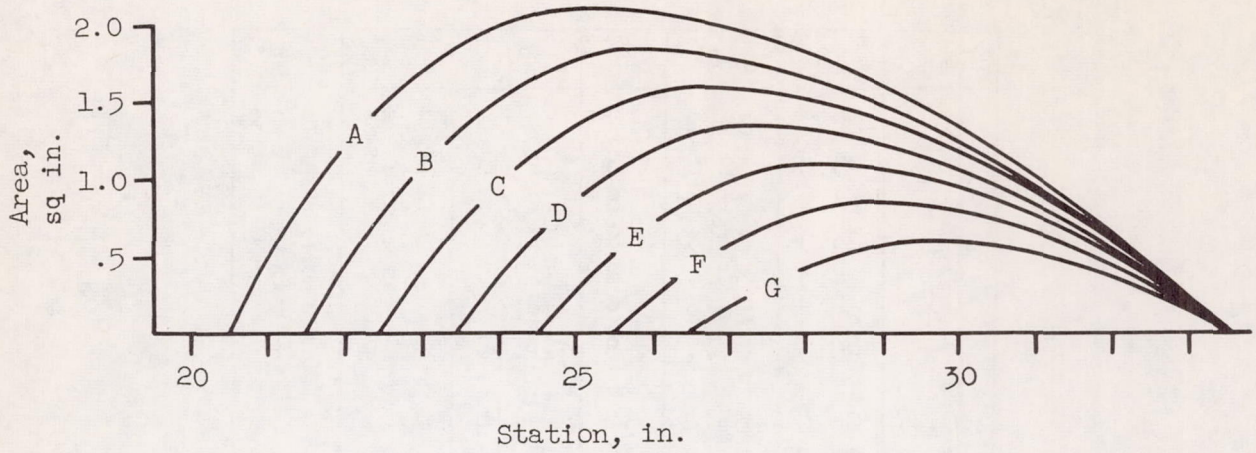

Each individual area plot is then further broken down into a number of rectangles, each rectangle being equal in frontal area. The leading and trailing edges of the rectangles are chosen to best represent the area progression of the particular area plot. These rectangles represent the elemental hoops upon which the computations are done.

The computational procedures may be carried out on a simple computation form as is shown below. The leading-edge and trailing-edge positions and the hoop radii are first reduced to dimensionless parameters. A sample computation showing this procedure is given for two families of hoops for a $M = 1.82$ ($\tan \mu = 0.66$).

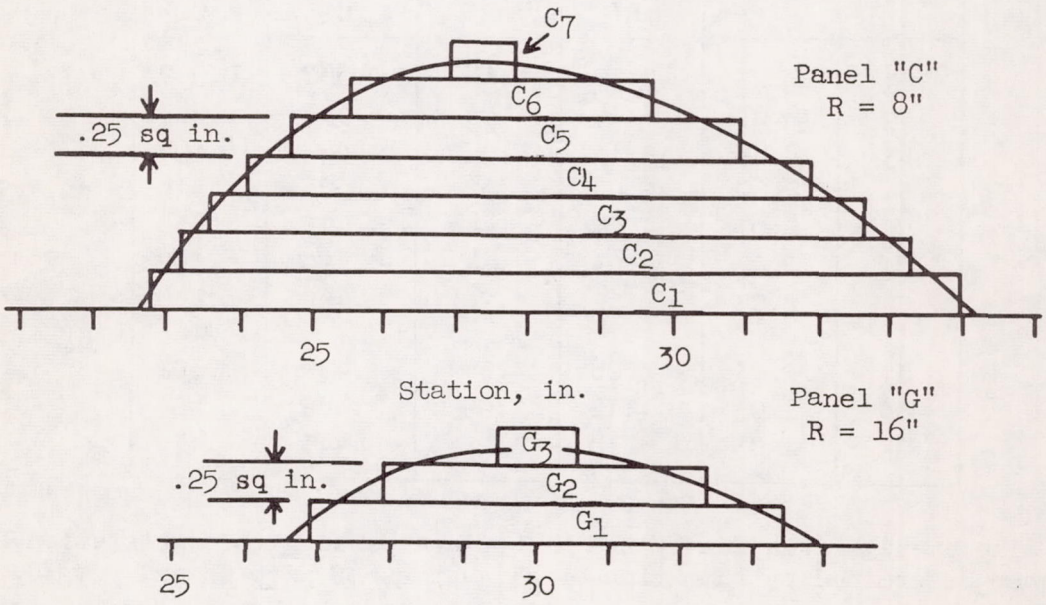

Hoop	L	T	R	R'	L/R'	T/R'
C_1	22.7	33.2	8	12.08	1.88	2.75
C_2	23.0	32.6	8	12.08	1.91	2.70
C_3	23.4	31.9	8	12.08	1.94	2.64
C_4	23.9	31.3	8	12.08	1.98	2.59
C_5	24.5	30.4	8	12.08	2.03	2.51
C_6	25.3	29.2	8	12.08	2.10	2.41
C_7	26.5	27.4	8	12.08	2.19	2.27
G_1	26.8	33.0	16	24.16	1.11	1.37
G_2	27.7	31.9	16	24.16	1.15	1.32
G_3	29.2	30.2	16	24.16	1.21	1.25

The area cut at any station X is next determined by first computing values of $\frac{L - X}{R'}$ and $\frac{T - X}{R'}$ and then determining C_{LE}/C and C_{TE}/C from a plot of these functions (fig. 10) or from equations (2) and (3). The computation for this is illustrated in the following table for station X = 25.

Hoop	X/R'	$\frac{L - X}{R'}$	$\frac{T - X}{R'}$	$\frac{C_{LE}}{C}$	$\frac{C_{TE}}{C}$
C_1	2.07	-0.19	0.68	0.562	0.262
C_2	2.07	-.16	.63	.552	.283
C_3	2.07	-.13	.57	.542	.307
C_4	2.07	-.09	.52	.523	.316
C_5	2.07	-.04	.44	.513	.356
C_6	2.07	.03	.34	.490	.392
C_7	2.07	.12	.20	.462	.436
G_1	1.03	.08	.34	.472	.392
G_2	1.03	.12	.29	.462	.407
G_3	1.03	.18	.22	.443	.430

The average area cut by the Mach plane passing through station 25 is then determined by summation of all values of C_{LE}/C and C_{TE}/C. The difference between these summations multiplied by the frontal area of the elemental hoops (0.25 sq in. for this case) is the projected

frontal area cut by the Mach plane. This may be expressed as follows:

$$A = A^*\left(\sum \frac{C_{LE}}{C} - \sum \frac{C_{TE}}{C}\right)$$

For the design of indented configurations, according to the area-rule concept, the indentations are obtained by subtracting the summed projected area of the wing from the body cross-sectional area at corresponding stations.

REFERENCES

1. Whitcomb, Richard T.: A Study of the Zero-Lift Drag-Rise Characteristics of Wing-Body Combinations Near the Speed of Sound. NACA RM L52H08, 1952.

2. Hoffman, Sherwood: A Flight Investigation of the Transonic Area Rule for a 52.5° Sweptback Wing-Body Configuration at Mach Numbers Between 0.8 and 1.6. NACA RM L54H13a, 1954.

3. Hoffman, Sherwood: An Investigation of the Transonic Area Rule by Flight Tests of a Sweptback Wing on a Cylindrical Body With and Without Body Indentation Between Mach Numbers 0.9 and 1.8. NACA RM L53J20a, 1953.

4. Hall, James Rudyard: Comparison of Free-Flight Measurements of the Zero-Lift Drag Rise of Six Airplane Configurations and Their Equivalent Bodies of Revolution at Transonic Speeds. NACA RM L53J21a, 1954.

5. Robinson, Harold L.: A Transonic Wind-Tunnel Investigation of the Effects of Body Indentation, As Specified by the Transonic Drag-Rise Rule, on the Aerodynamic Characteristics and Flow Phenomena of a 45° Sweptback-Wing—Body Combination. NACA RM L52L12, 1953.

6. Carmel, Melvin M.: Transonic Wind-Tunnel Investigation of the Effects of Aspect Ratio, Spanwise Variations in Section Thickness Ratio, and a Body Indentation on the Aerodynamic Characteristics of a 45° Sweptback Wing-Body Combination. NACA RM L52L26b, 1953.

7. Williams, Claude V.: A Transonic Wind-Tunnel Investigation of the Effects of Body Indentation, As Specified by the Transonic Drag-Rise Rule, on the Aerodynamic Characteristics and Flow Phenomena of an Unswept-Wing—Body Combination. NACA RM L52L23, 1953.

8. Wornom, Dewey E., and Osborne, Robert S.: Effects of Body Indentation on the Drag Characteristics of a Delta-Wing—Body Combination at Transonic Speeds. NACA RM L54K12a, 1954.

9. Whitcomb, Richard T.: Recent Results Pertaining to the Application of the "Area Rule." NACA RM L53I15a, 1953.

10. Hopko, Russell N., Piland, Robert O., and Hall, James R.: Drag Measurements at Low Lift of a Four-Nacelle Airplane Configuration Having a Longitudinal Distribution of Cross-Sectional Area Conducive to Low Transonic Drag Rise. NACA RM L53E29, 1953.

11. Carlson, Harry W.: Preliminary Investigation of the Effects of Body Contouring As Specified by the Transonic Area Rule on the Aerodynamic Characteristics of a Delta Wing-Body Combination at Mach Numbers of 1.41 and 2.01. NACA RM L53G03, 1953.

12. Whitcomb, Richard T., and Fischetti, Thomas L.: Development of a Supersonic Area Rule and an Application to the Design of a Wing-Body Combination Having High Lift-to-Drag Ratios. NACA RM L53H31a, 1953.

13. Jones, Robert T.: Theory of Wing-Body Drag at Supersonic Speeds. NACA RM A53H18a, 1953.

14. Holdaway, George H.: Comparison of Theoretical and Experimental Zero-Lift Drag-Rise Characteristics of Wing-Body-Tail Combinations Near the Speed of Sound. NACA RM A53H17, 1953.

15. Alksne, Alberta: A Comparison of Two Methods for Computing the Wave Drag of Wing-Body Combinations. NACA RM A55A06a, 1955.

16. Morrow, John D., and Nelson, Robert L.: Large-Scale Flight Measurements of Zero-Lift Drag of 10 Wing-Body Configurations at Mach Numbers From 0.8 to 1.6. NACA RM L52D18a, 1953.

17. Wallskog, Harvey A., and Hart, Roger G.: Investigation of the Drag of Blunt-Nosed Bodies of Revolution in Free Flight at Mach Numbers From 0.6 to 2.3. NACA RM L53D14a, 1953.

18. Hayes, Wallace D.: Linearized Supersonic Flow. Rep. No. AL-222, North American Aviation, Inc., June 18, 1947, pp. 94-95.

TABLE I

COORDINATES OF NACA 65A004.5 AIRFOIL

Station, percent chord	Ordinate, percent chord
0	0
.5	.349
.75	.424
1.25	.540
2.5	.738
5.0	.986
7.5	1.194
10	1.368
15	1.646
20	1.855
25	2.014
30	2.131
35	2.208
40	2.246
45	2.245
50	2.196
55	2.099
60	1.957
65	1.780
70	1.572
75	1.338
80	1.084
85	.818
90	.549
95	.280
100	.010
L.E. radius: 0.130 percent chord T.E. radius: 0.0115 percent chord	

TABLE II

COORDINATES OF PARABOLIC BODY[1]

[Stations measured from body nose]

Station, in.	Ordinate, in.
0	0
1	.245
2	.481
4	.923
6	1.327
10	2.019
14	2.558
18	2.942
22	3.173
26	3.250
30	3.233
34	3.181
38	3.095
42	2.975
46	2.820
50	2.631
54	2.407
58	2.149
62	1.857
65	1.615

[1]Based on length of the 65-inch body.

TABLE III

COORDINATES OF BODY WITH MACH NUMBER 1.10 INDENTATION

[Stations measured from body nose]

Station, in.	Ordinate, in.
(a)	(a)
30	3.233
32	3.160
34	2.920
36	2.650
38	2.375
40	2.185
42	2.095
44	2.108
46	2.185
48	2.272
50	2.348
52	2.402
54	2.375
56	2.285
58	2.149
60	2.007
62	1.857
64	1.698
65	1.615

[a]Coordinates between stations 0 and 30 are identical to those of table II.

TABLE IV

COORDINATES OF BODY WITH MACH NUMBER 1.41 INDENTATION

[Stations measured from body nose]

Station, in.	Ordinate, in.
(a)	(a)
22	3.173
24	3.190
26	3.175
28	3.140
30	3.080
32	2.985
34	2.870
36	2.742
38	2.642
40	2.560
42	2.482
44	2.422
46	2.368
48	2.325
50	2.288
52	2.252
54	2.220
56	2.152
58	2.042
60	1.932
62	1.790
64	1.650
65	1.610

[a]Coordinates between stations 0 and 22 are identical to those of table II.

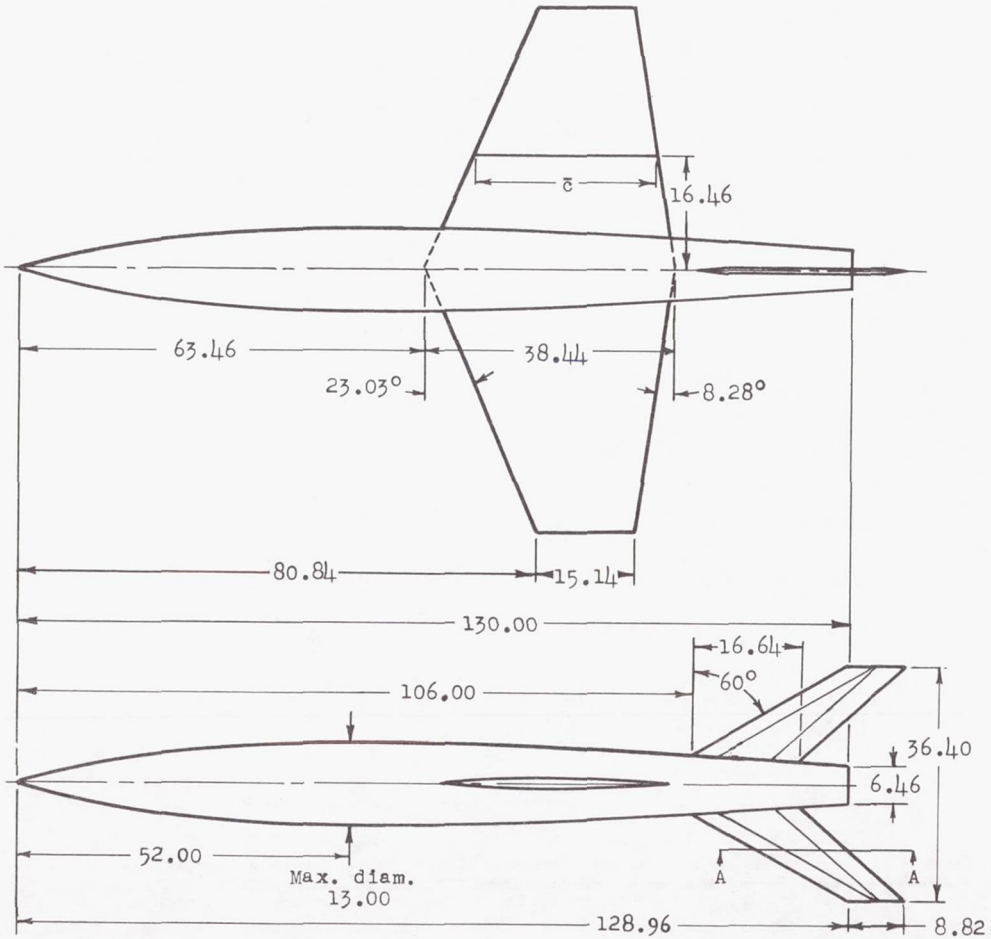

Model Characteristics

Wing aspect ratio	3.04
Wing taper ratio	0.394
Wing mean aerodynamic chord, ft	2.375
Free stream airfoil, NACA 65A004.5	Table I
Total wing planform area, sq ft	15.208
Body fineness ratio	10.0
Body frontal area, sq ft	0.922
Body coordinates, Model A	Table II

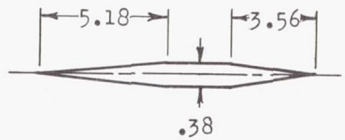

A-A
Typical fin section

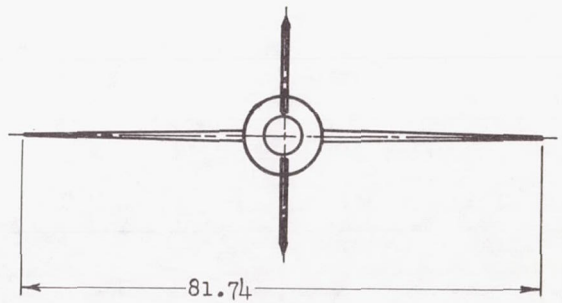

(a) Basic wing-body combination (ref. 16). Model A.

Figure 1.- Details and dimensions of models. All dimensions are in inches.

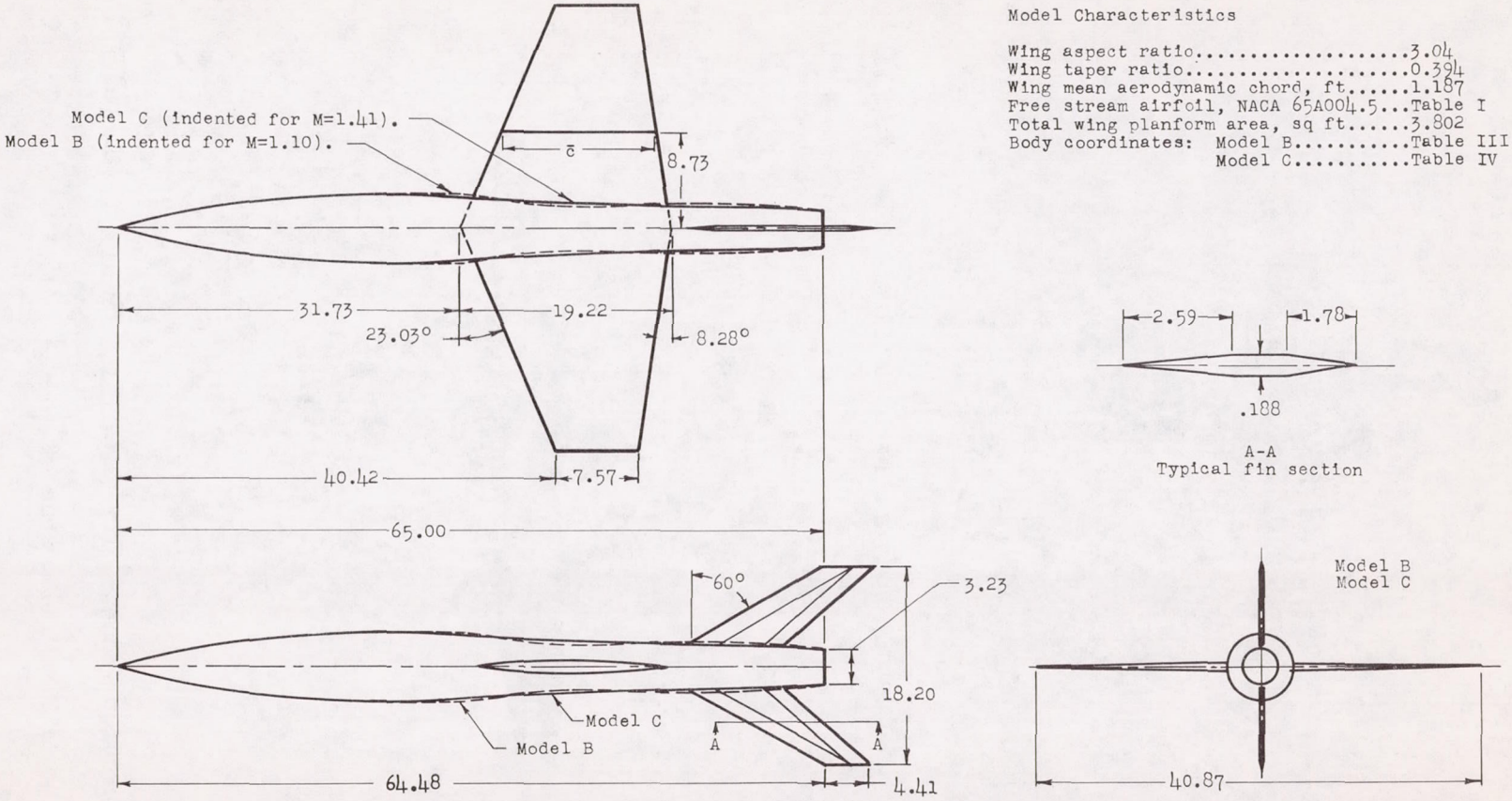

(b) Configurations with body indentation for Mach number 1.10 and 1.41. Model B and Model C.

Figure 1.- Concluded.

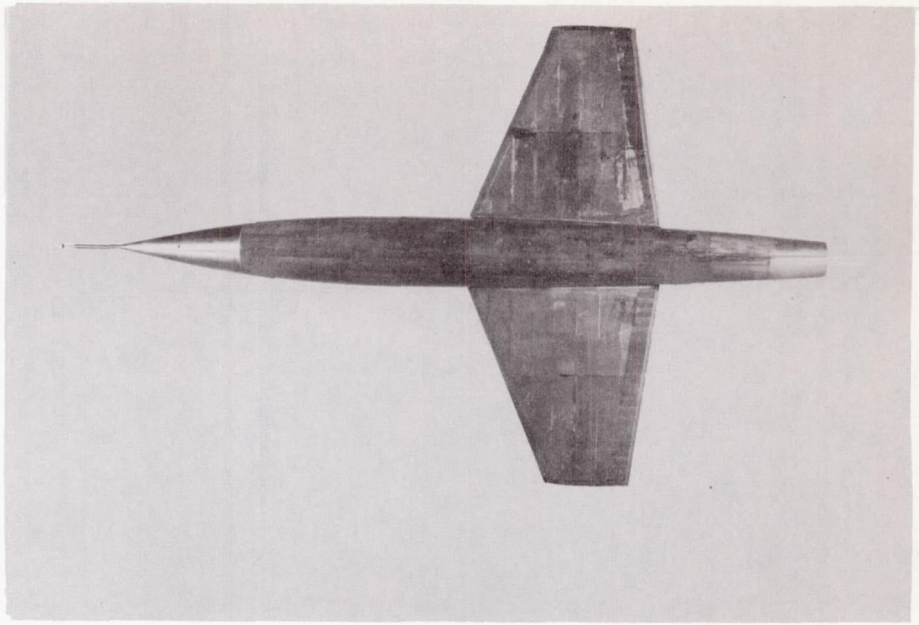

(a) Basic configuration (ref. 16). Model A. L-72147.1

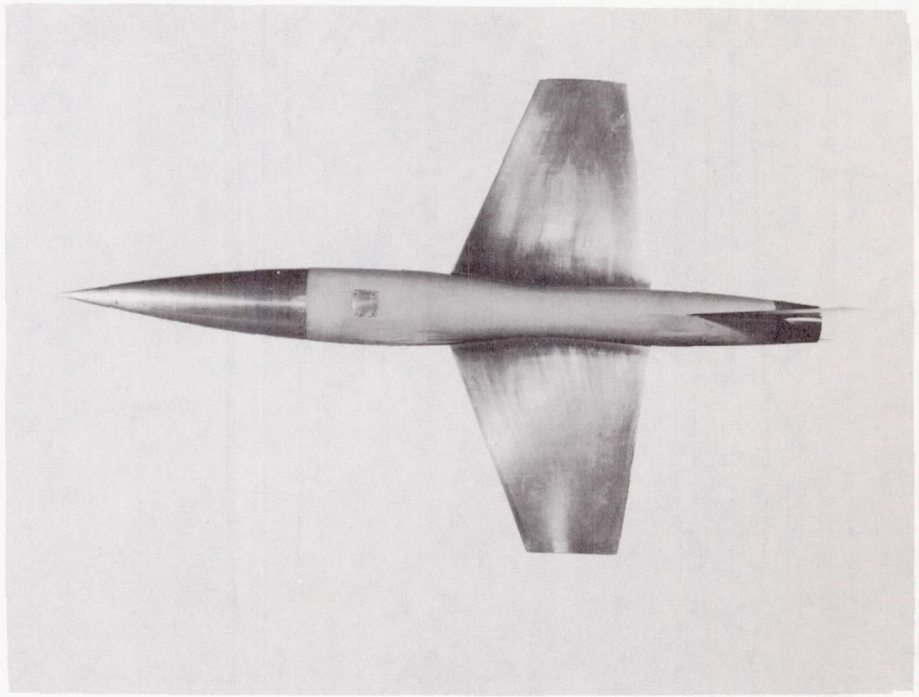

(b) Configuration indented for M = 1.10. Model B. L-84557.1

Figure 2.- Photographs of models.

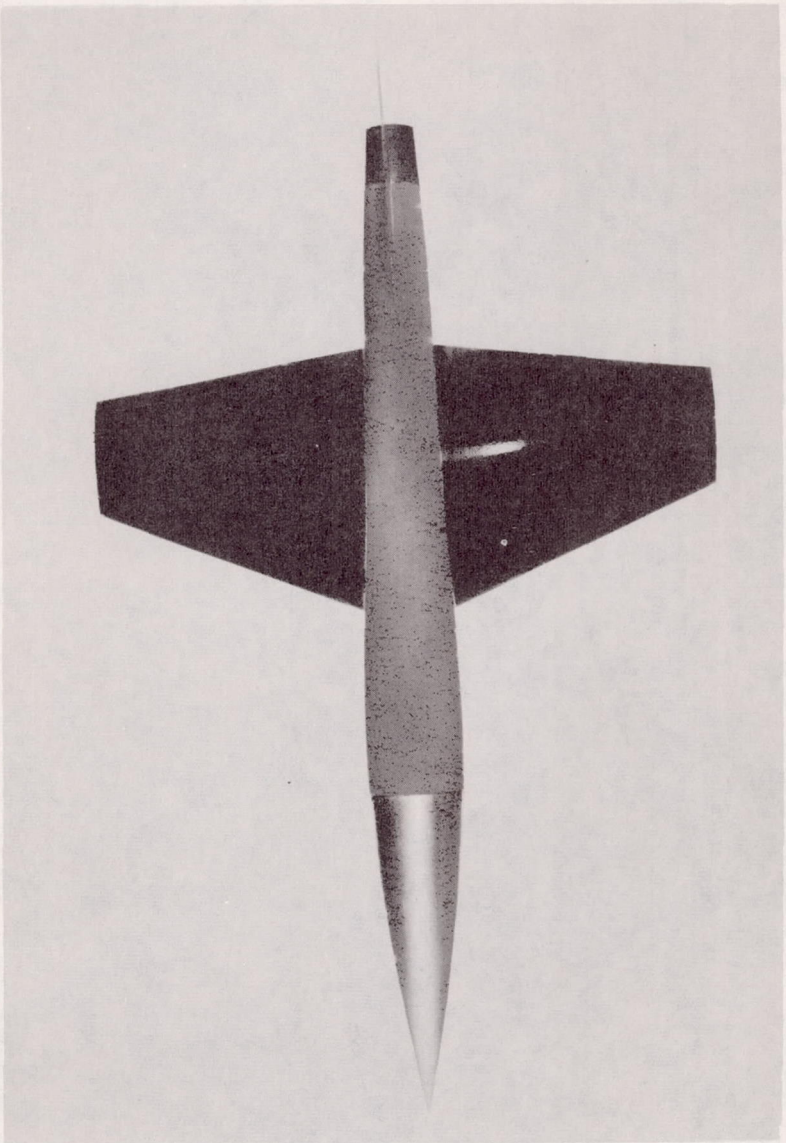

(c) Configuration indented for M = 1.41. Model C. L-84433.1

Figure 2.- Concluded.

L-84685.1

Figure 3.- Photograph of a model and booster on zero-length launcher.

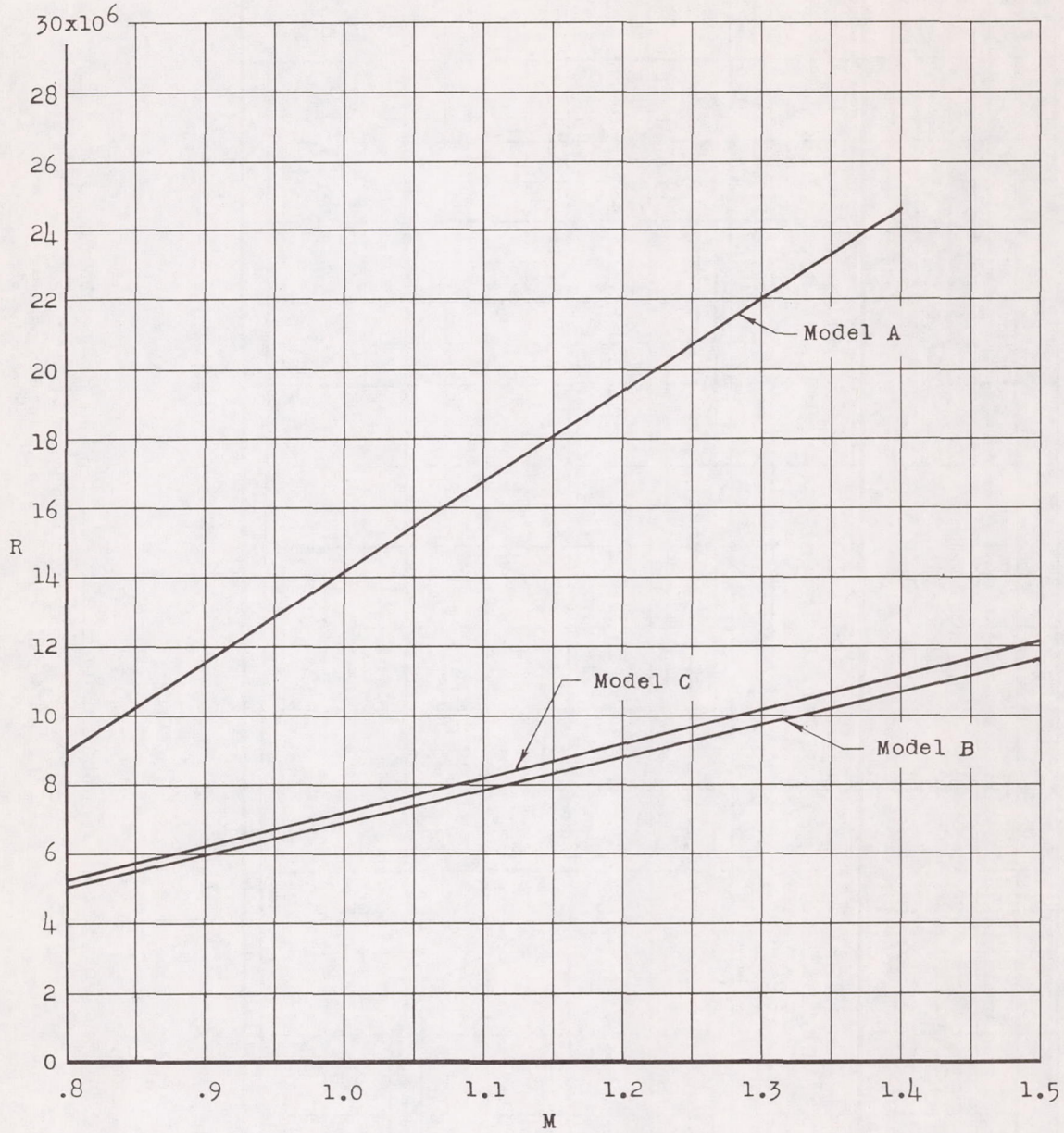

Figure 4.- Variation of Reynolds number with Mach number. Reynolds number is based on the mean aerodynamic chord of the wing.

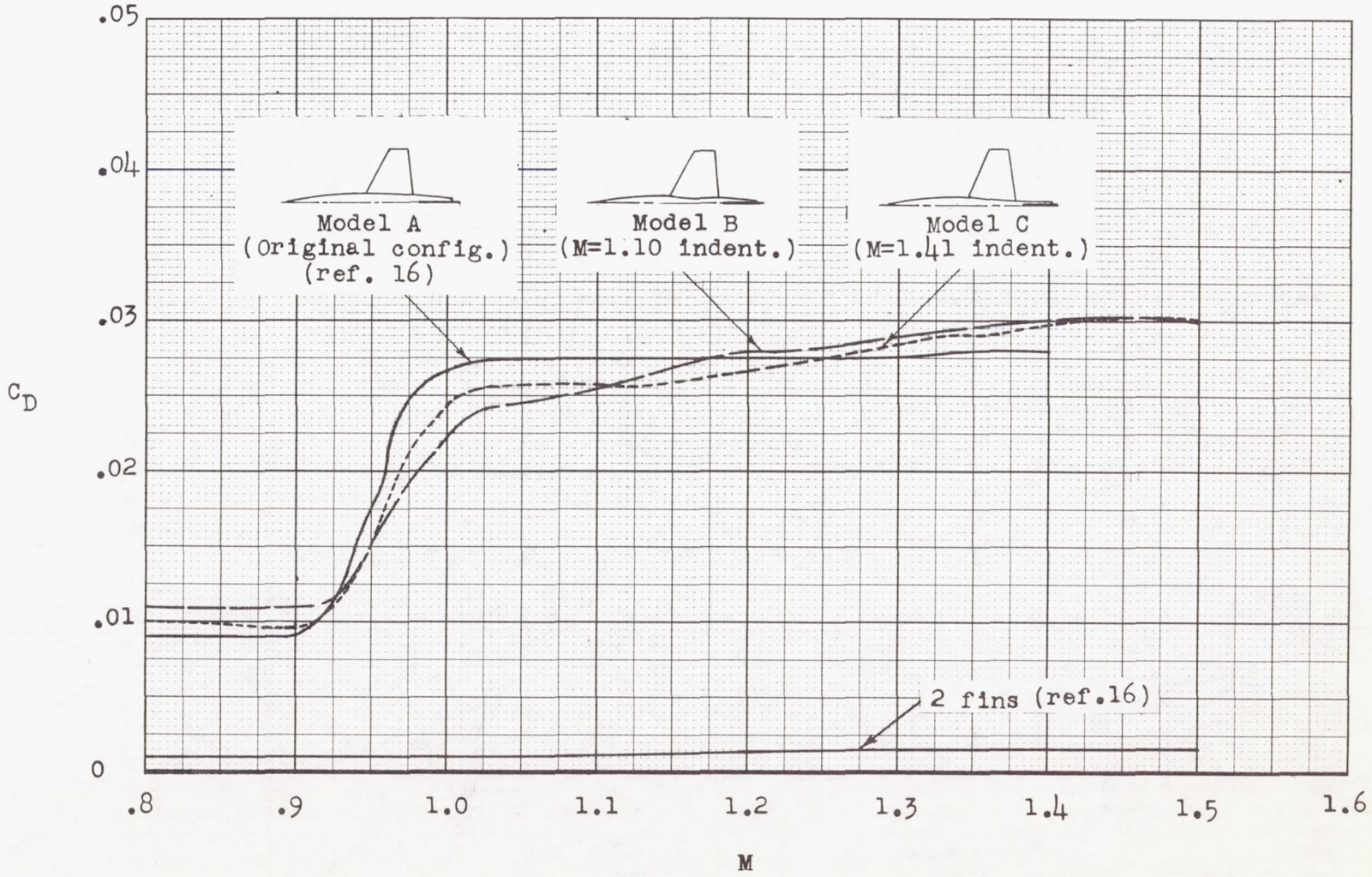

Figure 5.- Variation of total drag coefficient with Mach number for models tested.

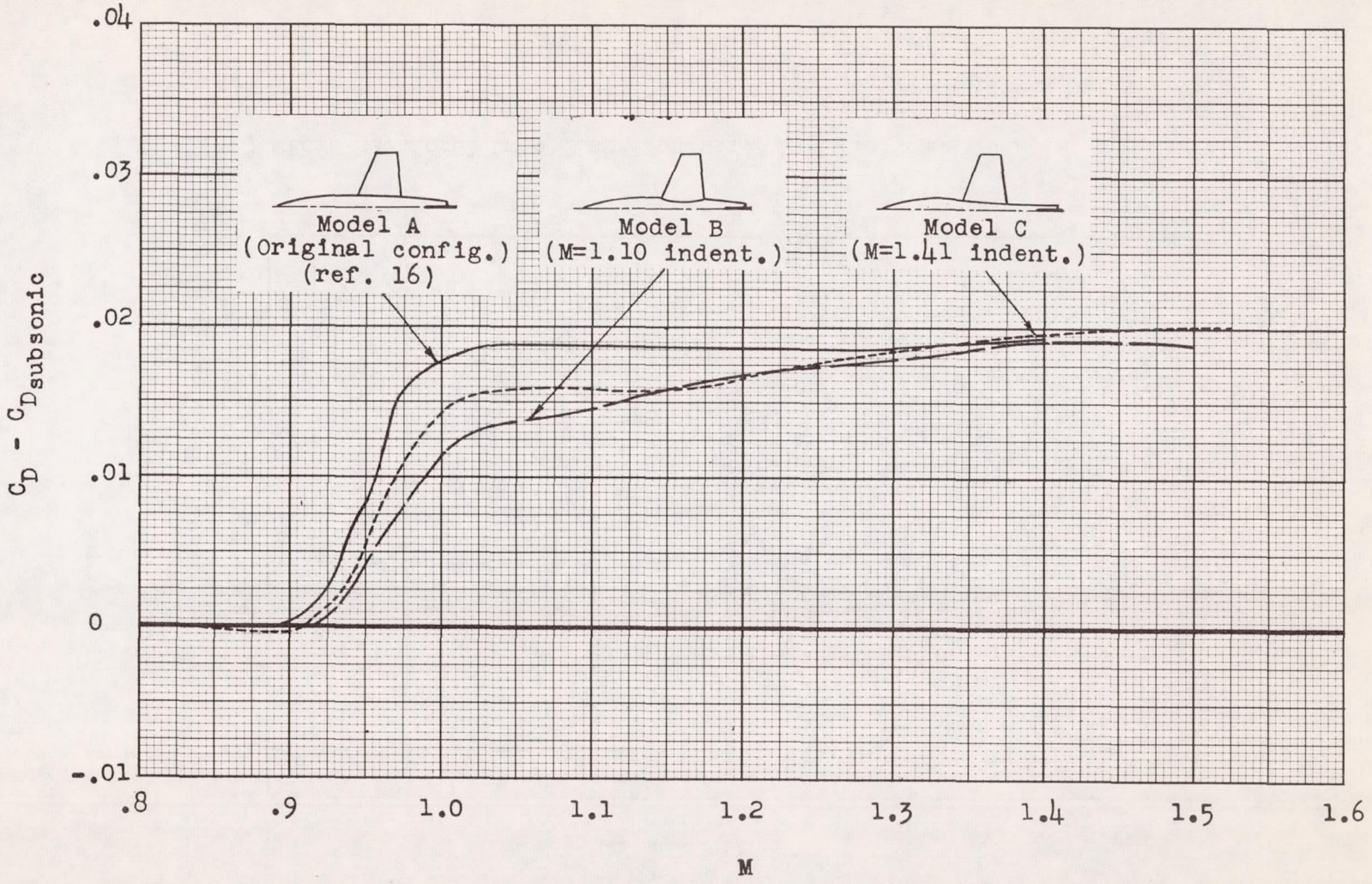

Figure 6.- Comparison of the variation of drag rise coefficient with Mach number for models tested.

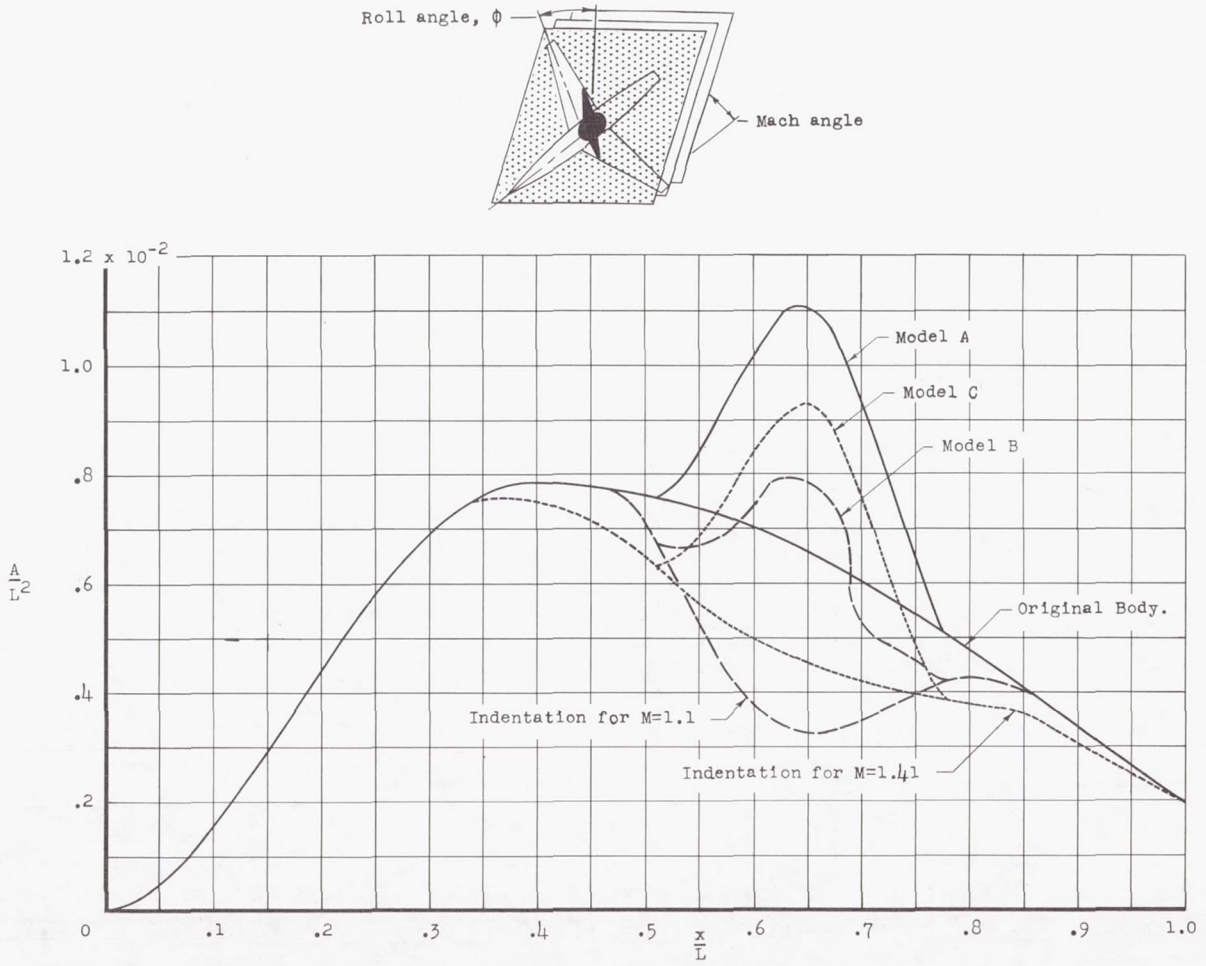

(a) Cross-sectional area distributions. M = 1.0. Models A, B, and C.

Figure 7.- Comparisons of area distributions of models tested at various Mach numbers.

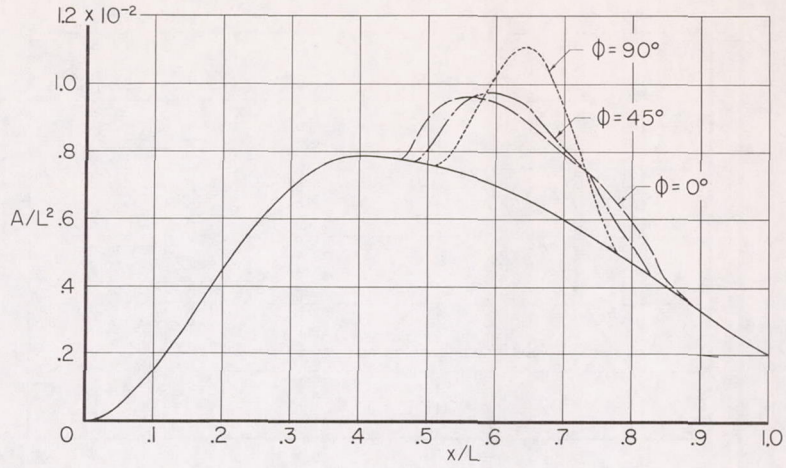

(b) Basic configuration at M = 1.10. Model A.

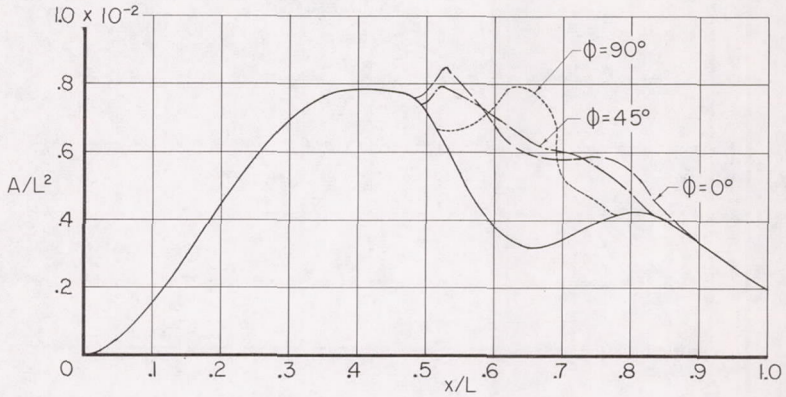

(c) Configuration indented for Mach number 1.10 at M = 1.10. Model B.

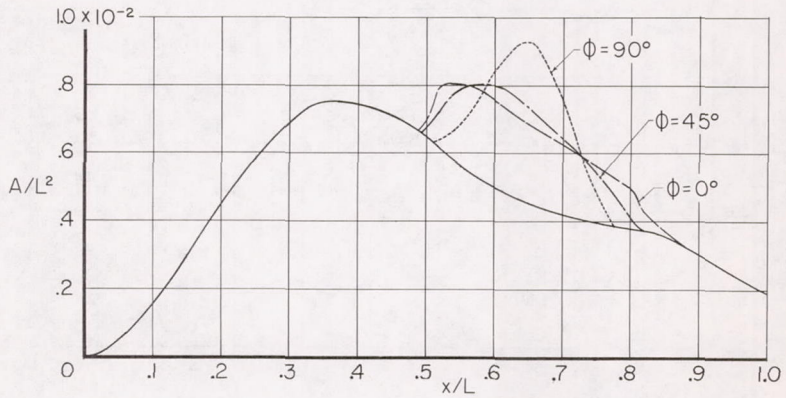

(d) Configuration indented for Mach number 1.41 at M = 1.10. Model C.

Figure 7.- Continued.

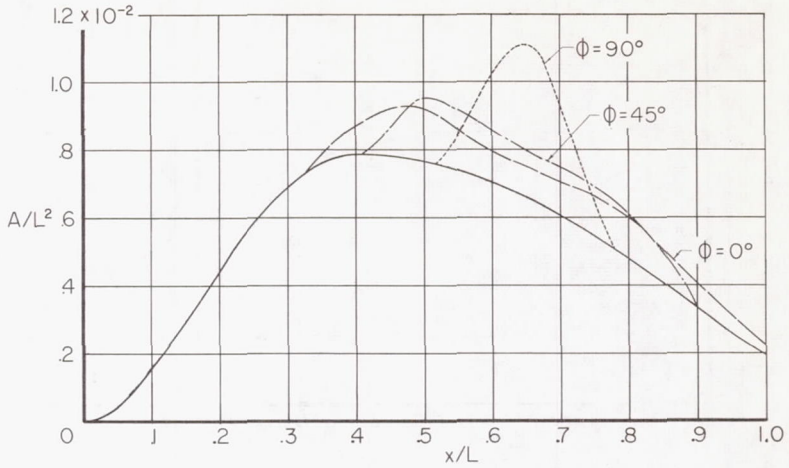

(e) Basic configuration at M = 1.41. Model A.

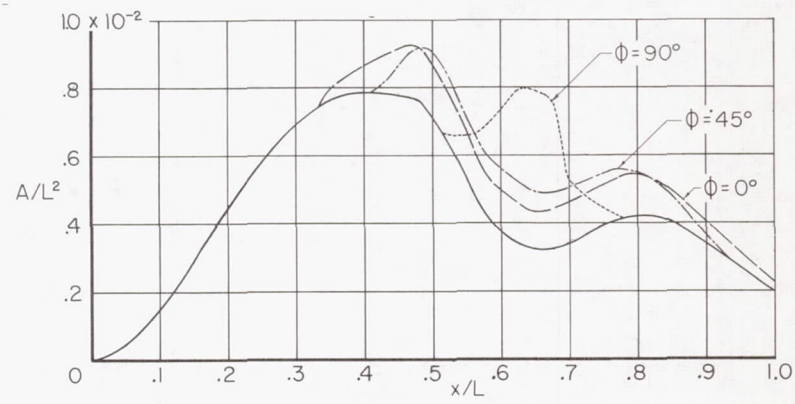

(f) Configuration indented for Mach number 1.10 at M = 1.41. Model B.

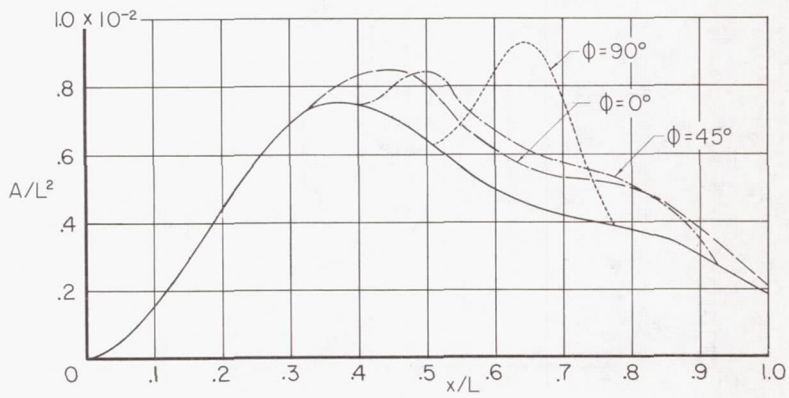

(g) Configuration indented for Mach number 1.41 at M = 1.41. Model C.

Figure 7.- Concluded.

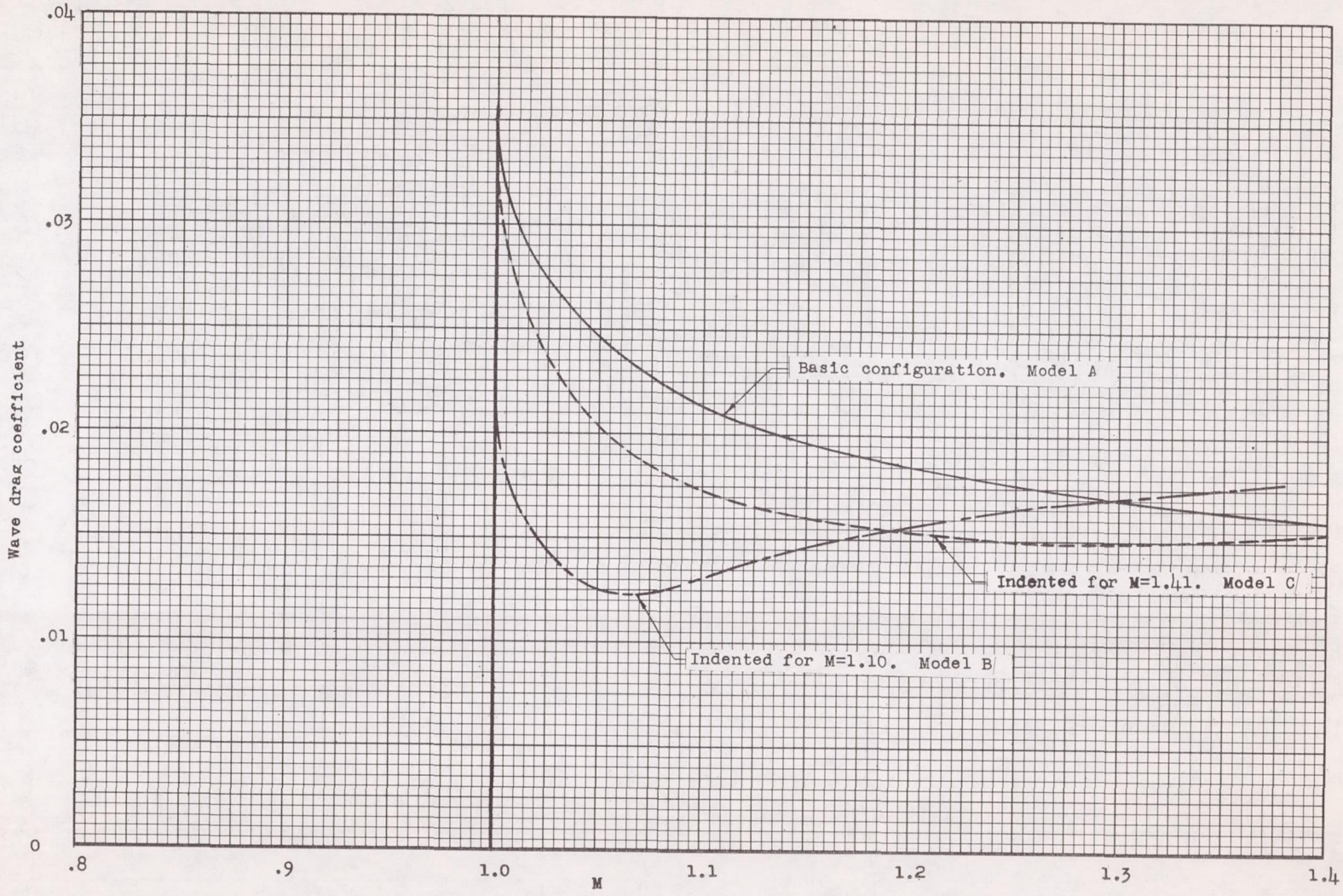

Figure 8.- Comparison of the variation of the theoretical wave drag coefficients with Mach number for models A, B, and C.

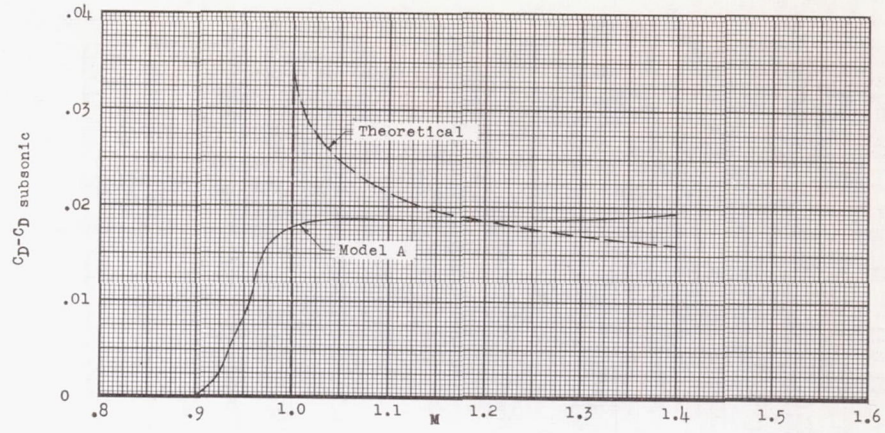

(a) Basic configuration.

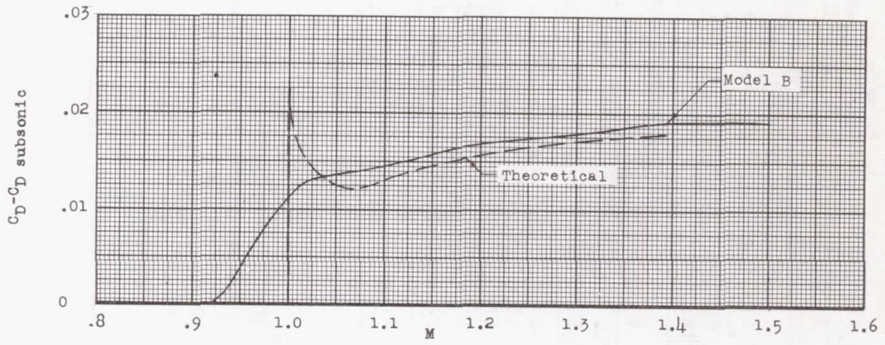

(b) Configuration indented for M = 1.10.

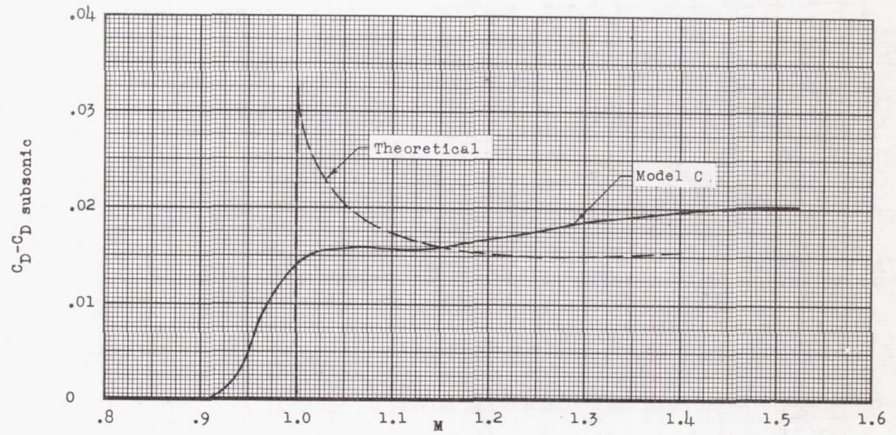

(c) Configuration indented for M = 1.41.

Figure 9.- Comparison of the measured drag rise coefficient and the theoretical wave drag coefficient for each model tested.

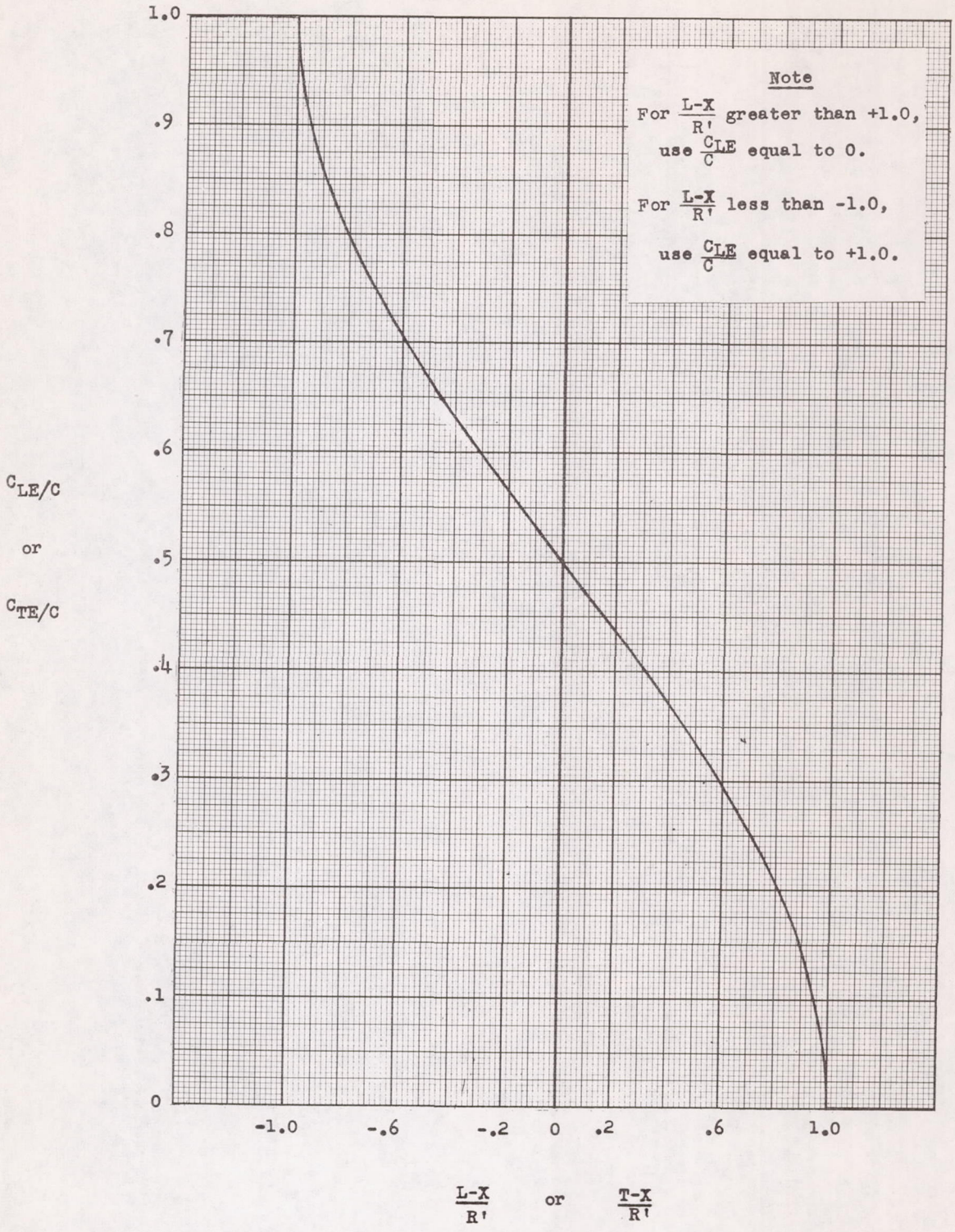

Figure 10.- Variation of area parameters for use with computational procedure given in appendix.